Naturally occurring eugenin: Biosynthesis, distribution, bioactivity, and therapeutic potential

Lutfun Nahar[1]*, Waed Alsheikh[2], Kenneth J. Ritchie[2], Satyajit D. Sarker[2]*

[1]*Laboratory of Growth Regulators, Palacký University and Institute of Experimental Botany, The Czech Academy of Sciences, Šlechtitelů 27, 78371 Olomouc, Czech Republic*

[2]*Centre for Natural Products Discovery (CNPD), School of Pharmacy and Biomolecular Sciences, Liverpool John Moores University, James Parsons Building, Byrom Street, Liverpool L3 3AF, United Kingdom*

*Corresponding authors: nahar@ueb.cas.cz (L.N.) and S.Sarker@ljmu.ac.uk (S.D.S.)

Highlights:

- Eugenin belongs to the chromone class of natural products and has been reported from at least 22 different plant species from 13 families.
- Carrots and cloves are two major sources of eugenin.
- Eugenin has also been isolated from two fungal species, *Aschersonia confluens* and *Chaetomium minutum.*
- The biosynthesis of this compound follows the acetate-malonate pathway.
- Among several bioactivities, antioxidant, antiplatelet aggregation, immunosuppressive/immunomodulatory activities of eugenin and its *in silico* prediction of antiviral property against SARS-CoV-2 activity may have some therapeutic potential.

ABSTRACT

Introduction: Eugenin (5-hydroxy-7-methoxy-2-methyl-4H-chromen-4-one) is a bioactive phytoalexin mainly found as a bitter component in carrots (*Daucus carota* L.; Apiaceae) and cloves [*Syzygium aromaticum* (L.) Merr. & L. M. Perry; Myrtaceae].

Materials and methods: An extensive literature search was performed involving various established databases like Web of Science, PubMed, Science Direct, Dictionary of Natural Products and Google Scholar, using the keyword 'eugenin'. The literature reports that describe various aspects of naturally occurring eugenin, e.g., isolation, structure elucidation, biosynthesis, bioactivity studies and therapeutic potential, have been included in this review, while the papers that present total synthesis or structural modifications of eugenin have been excluded.

Results: Eugenin, biosynthesized from the acetate-malonate pathway, has been reported from at least 22 plant species from 13 families. It has also been found in two fungal species, *Aschersonia confluens* and *Chaetomium minutum*. *Dacaus carota* and *Syzygium aromaticum* are two major sources of this chromone. Antimalarial, antimicrobial, antioxidant, antiplatelet aggregation, antiviral, cytotoxic, immunosuppressive/immunomodulatory, osteogenesis-inducing, pyrolyl endopeptidase (PEP)-inhibitory and blue-green algae growth inhibitory activities of eugenin have been reported in the literature. Among these bioactivities, antioxidant, antiplatelet aggregation, immunosuppressive/immunomodulatory activities of eugenin and its *in silico* prediction of antiviral property against severe-acute-respiratory-syndrome-related coronavirus-2 (SARS-CoV-2) activity may have some therapeutic potential.

Conclusion: The distribution of eugenin is rather limited to a few plant species and only a couple of fungal species. Based on the reported bioactivities, it could be concluded that this chromone might have some potential as a template for new drug development.

Keywords: Anticancer; Bioactivity; Carrots; Chromones; Cloves; Eugenin; Nuclear Magnetic Resonance (NMR)

1. Introduction

Eugenin (5-hydroxy-7-methoxy-2-methyl-4H-chromen-4-one, **1**) (**Fig. 1**), molecular formula: $C_{11}H_{10}O_4$, molecular weight: 206.19, is a phytoalexin mainly found as a bitter component in carrots (*Daucus carota* L.; Apiaceae) and cloves [*Syzygium aromaticum* (L.) Merr. & L. M. Perry; Myrtaceae] (Meijer and Schmid, 1948; Stoessl and Stothers, 1978; Al-Douri and Dewick, 1988; Czepa and Hofmann, 2003). Eugenin (**1**), first isolated from *Syzygium aromaticum (alt. Eugenia caryophyllata* Thunb.) several decades ago (Meijer and Schmid, 1948), is known to be the biosynthetic precursor of several pharmacologically active molecules, e.g., the anti-asthmatic furochromones visnagin and kehellin found in *Ammi visnaga* (Morita et al., 2010). This chromone is also a bioactive compound with some therapeutic potential.

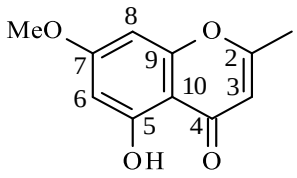

Fig. 1 Structure of eugenin (**1**)

The extraction process of eugenin (**1**) from plant matrices appears to be quite straightforward, and various organic solvents, e.g., ethanol (EtOH) and methanol (MeOH), could be used in simple extraction techniques like maceration, percolation and Soxhlet (Saito et al., 1989; Ali et al., 1990; Chang et al., 2003; Han and Paik, 2010; Najmuldeen et al., 2013; Anh et al., 2014; Kayed et al., 2021). The isolation of this compound mostly involves classical normal phase chromatography, e.g., column chromatography, vacuum liquid chromatography (VLC), gel filtration (Sephadex) and solvent partitioning (Saito et al., 1989; Ali et al., 1990; Rao et al., 1991; Chang et al., 2003; Najmuldeen et al., 2013; Anh et al., 2014; Kayed et al., 2021), and the use of high-performance liquid chromatography (HPLC) could also be noticed in some studies (Czepa and Hofmann, 2003; Han and Paik, 2010).

Several published papers describe structure elucidation of this chromone using spectroscopic means, especially applying 1D and 2D NMR spectroscopic data analysis (**Tables 1** and **2**) (Coxon et al., 1973; Ali et al., 1990; Rao et al., 1991; Tsui and Brown, 1996; Czepa and Hofmann, 2003; Tuntiwachuttikul et al., 2006; Najmuldeen et al., 2013; Sadorn et al., 2020; Kayed et al., 2021). Three deuterated NMR solvents, i.e., $CDCl_3$, acetone-d_6 and CD_3OD

have been used to obtain all these NMR data, but $CDCl_3$ appears to be the most popular choice. However, there are significant differences in the assignment of all ^{1}H and ^{13}C NMR data, albeit eugenin (**1**) is rather a small phenolic compound (**Tables 1** and **2**). The differences in reported chemical shift assignments among various papers could be a result of the absence of required 2D NMR data, incorrect calibration of the residual solvent peak or simply just typographical errors. Therefore, the authors' unpublished and unequivocally assigned ^{1}H and ^{13}C NMR data, based on extensive 1D and 2D NMR analyses, obtained in CD_3OD, have been included in **Tables 1** and **2**.

Although eugenin (**1**) was isolated during the first half of the 20th century, and a fair number of studies have been carried out since its first isolation, to the best of our knowledge, there is no review article published on eugenin (**1**). This mini-review appraises all published data on naturally occurring eugenin (**1**), including its natural distribution, biosynthesis, and bioactivity.

2. Natural sources

Although *Dacaus carota*, *Pisonia aculeata* L. (fam: Nyctagenaceae) and *Syzygium aromaticum* are the major plant sources of eugenin (**1**), this chromone is distributed in a few other plants, e.g., *Crossosoma bigelovii* S. Wats. (fam: Crossosomataceae) and *Pogostemon stellatus* (Lour.) Kuntze (fam: Lamiaceae) (Al-Douri and Dewick, 1988; Morita et al., 2010; ChEBI, 2023; PubChem, 2023), as well as other organisms, e.g., the fungus *Aschersonia confluencs* BCC53152 (Sadorn et al., 2020) (**Table 3**). Based on the published literature, there are at least 22 plant species from 13 families and two fungal species that produce eugenin (**1**). Among the plant families, the Apiaceae appears to be the best source of this chromone. Plants from other families, e.g., Amaryllidaceae, Crossosomataceae, Fabaceae, Haloragaceae, Iridaceae, Lamiaceae, Meliaceae, Myrtaceae, Nyctagenaceae, Rubiaceae, Rutaceae, Solanaceae and Trapaceae, have been reported to biosynthesize eugenin (**1**) (**Table 3**). While plant root, e.g., *D. carota* root, tends to accumulate eugenin (**1**) in high concentration, this chromone has also been reported from other plant parts, e.g., flower, bud, bulb, leaf, seed, and stem.

Table 1. ^{1}H NMR data in different deuterated solvents as reported in the literature

Position	^{1}H NMR chemical shift (δ) in ppm (coupling constant *J* in Hz)									
	$CDCl_3$						Acetone-d_6	CD_3OD		
	Coxon et al., 1973	Ali et al. 1990	Rao et al., 1991	Tsui & Brown, 1996	Czepa & Hofmann, 2003	Najmuldeen et al., 2013	Sadorn et al., 2020	Han & Paik, 2010	Kayed et al., 2021	Unpublished**
3	6.14, *s*, 1H	6.00, *s*, 1H	6.00, *s*, 1H	6.02, *s*, 1H	6.02, *s*, 1H	6.00, *s*, 1H	6.10, *s*, 1H	5.99, *s*, 1H	5.94, *s*, 1H	6.09, *s*, 1H
6	6.36, *s****	6.31, *d* (2.2), 1H	6.31, *d* (2.0), 1H	6.33, 1H	6.33, *d* (2.2), 1H	6.30, *d* (2.0), 1H	6.34, *d* (1.9), 1H	6.29, *d* (2.0), 1H	6.06, *br s*, 1H*	6.32, *br s*, 1H*
8	6.36, *s****	6.33, *d* (2.2), 1H	6.33, *d* (2.0), 1H	6.35, 1H	6.36, *d* (2.2), 1H	6.33, *d* (2.0), 1H	6.50, *d* (1.9), 1H	6.31, *d* (2.0), 1H	6.18, *br s*, 1H*	6.49, *br s*, 1H*
2-Me	2.34, *s*, 3H	2.33, *s*, 3H	2.33, *s*, 3H	2.15, *s*, 3H	2.34, *s*, 3H	2.34, *s*, 3H	2.39, *s*, 3H	2.32, *s*, 3H	2.25, *s*, 3H	2.37, *s*, 3H
5-OH	7.33, *s*, 1H	12.68, *s*, 1H	12.70, *br s*, 1H	12.69, *s*, 1H	12.68, *s*, 1H	12.69, *s*, 1H	12.80, *s*, 1H		-	-
7-OMe	3.85, *s*, 3H	3.84, *s*, 3H	3.83, *s*, 3H	3.85, *s*, 3H	3.85, *s*, 3H	3.84, *s*, 3H	3.88, *s*, 3H	3.82, *s*, 3H	3.75, *s*, 3H	3.85, *s*, 3H

*Unresolved peak, identified from COSY correlations.
**Unpublished data from authors' own work providing unequivocal assignment of all ^{1}H NMR signals using 1D and 2D experiments; ^{1}H NMR (600 MHz)
***Integrated for 2H

Table 2. ^{13}C NMR data in different deuterated solvents as reported in the literature

Position	^{13}C NMR chemical shift (δ) in ppm									
	$CDCl_3$						Acetone-d_6	CD_3OD		
	Ali et al., 1990	Rao et al., 1991	Tsui and Brown, 1996	Czepa and Hofmann, 2003	Tuntiwachuttikul et al., 2006	Najmuldeen et al., 2013	Sadorn et al., 2020	Han & Paik, 2010	Kayed et al., 2021	Unpublished*
2	158.1	165.4	166.8	158.1	166.8	166.9	168.6	166.6	148.2	168.3
3	108.8	108.7	105.9	108.8	106.9	108.8	109.1	108.7	109.3	107.8
4	182.5	182.4	183.1	182.5	182.5	182.6	183.2	182.3	183.9	182.7
5	165.4	162.2	160.2	165.4	162.2	162.2	163.0	162.0	164.5	161.7
6	97.9	98.0	97.9	97.9	97.8	98.0	98.5	97.8	99.3	97.7
7	166.8	166.6	163.0	166.8	165.4	165.4	166.4	165.1	168.9	165.9
8	92.5	92.4	92.5	92.5	92.5	92.5	92.9	92.4	93.7	92.0
9	162.2	158.1	155.0	162.3	158.1	158.2	159.0	157.9	160.6	158.4
10	105.2	105.2	104.7	105.3	105.5	105.5	105.6	105.1	105.1	104.5
2-Me	20.5	20.4	20.5	22.7	20.5	20.6	20.3	20.6	20.2	18.9
7-OMe	55.7	55.7	55.7	55.7	55.7	55.8	56.3	55.8	56.0	55.1

*Unpublished data from authors' own work providing unequivocal assignment of all ^{13}C NMR signals using 1D and 2D experiments; ^{13}C NMR (150 MHz)

Table 3. Natural sources of eugenin (**1**)

Sources	Family	Parts examined	Common names	References
Plants				
Acacia etbaica Schweinf.	Fabaceae	Leaf	Acacia in English, Arrad in Arabic	Kayed et al., 2021
Bupleurum scorzonerifolium Willd.	Apiaceae	Root	Bupleurum	Chang et al., 20023
Capsicum sp.	Solanaceae	Fruit	Chili	Yap et al., 2023
Crossosoma bigelovii S. Wats.	Crossosomataceae	Root	Ragged rockflower	Zhou, 2000; Klausmeyer et al., 2009
Daucus carota L.	Apiaceae	Root	Carrot	Sarker and Phan, 1979; Czepa and Hofmann, 2003
Daucus pumilus (L.) Hoffmann. & Link	Apiaceae	Root	Gouan, Dune carrot, Small carrot	Arafa et al., 2020
Dysoxylum macrocarpum Blume	Meliaceae	Leaf and bark	Jarum jarum	Najmuldeen et al., 2013
Gladiolus gandavensis Van Houtt.	Iridaceae	Subterranean rhizome	Sword lilies	Wang et al., 2003
Harrisonia perforata (Blanco) Merr.	Rutaceae	Brunch	Liana	Tuntiwachwuttikul et al., 2006
Hymenocallis littoralis Salisb.	Amaryllidaceae	Root	Beach spider lily	Anh et al., 2014
Ligusticum pteridophyllum Franch.	Apiaceae	Aerial parts	Ligusticum	Rao et al., 1991
Myriophyllum brasiliense Cambess.	Haloragaceae	Leaf	Red-stemmed parrots feather	Saito et al., 1989

Nauclea orientalis L.	Rubiaceae	Stem	Yellow chestwood	Fujita et al., 1967
Pancratium maritimum L.	Amaryllidaceae	Rhizome/bulb	Sea daffodil	Ali et al., 1990
Peucedanum japonicum Thunb.	Apiaceae	Root	Coastal hog fennel	Chen et al., 1996
Phaseolus multiflorus L. var, *albus*	Fabaceae	Bean	White kidney beans	Lee et al., 2023
Pimpinella anisum L.	Apiaceae	Cell culture	Aniseed	Soto-Argel et al., 2018
Pisonia aculeata L.	Nyctagenaceae	Leaf	Pisonia or Akobowere	ChEBI, 2023
Pogostemon stellatus (Lour.) Kuntze	Lamiaceae	Root	Pogostemon or Water star	Al-Douri and Dewick, 1988; Morita et al., 2010; PubChem, 2023
Schumanniphyton problematicum (A. Chev.) Aubrev.	Rubiaceae	Root	African Schumanniphyton	Schlittler and Spitaler, 1978
Syzygium aromaticum (L.) Merr. & L. M. Perry [*alt. Eugenia caryophyllata* Thunb.]	Myrtaceae	Buds and seeds	Cloves	Han and Paik, 2010; Ajiboye et al., 2016
Syzygium cumini (L.) Skeels.	Myrtaceae	Seed	Malabar plum or Java plum	Aeri et al., 2020
Fungus				
Aschersonia confluens Henn.	Clavicipitaceae	Fungal cells	Aschersonia fungus	Sadorn et al., 2020
Chaetomium minutum Krzemieniewska & Badura	Chaetomiaceae	Fungal cells	Dark-walled mold	Hauser and Zardin, 1972

3. Biosynthesis

Chromones are widespread in nature. However, the distribution of eugenin (**1**) is rather limited to a few plant families (**Table 3**). Most of these natural chromones possess a substituent at C-2, e.g., a methyl substituent at C-2 of eugenin (**1**), and they are good examples of polyketide structures that originate from the acetate-malonate pathway (Vickery and Vickery, 1981). Like most of the other chromones, the biosynthesis of eugenin (**1**) also follows the acetate-malonate pathway (Sarkar and Phan, 1975; Stoessl and Stothers, 1978; Morita et al., 2010) (**Fig. 2**). Pentaketide chromone synthase (PCS) catalyzes the biosynthesis of eugenin (**1**) through a five-step decarboxylative condensation of malonyl-CoA, followed by the Claisen 6-1 cyclization and methyl transferase catalyzed methylation of the C-7 hydroxyl functionality (**Fig. 2**). PCS may also, to a lesser extent, accept acetyl-CoA, which is the product of decarboxylation of malonyl-CoA, as a starter substrate. It, however, cannot be ascertained whether the ring closure is enzymatic or a result of spontaneous Michael-like ring closure. 5,7-Dihydroxy-2-methylchromone (also known as noreugenin) (**Fig. 2**) was found to be the biosynthetic precursor of eugenin (**1**) in the acetate-malonate pathway. The involvement of malonyl-CoA for the biosynthesis of eugenin (**1**) was demonstrated when a biotechnological approach was adopted by tailoring *Corynebacterium glutamicum* towards increased malolyl-CoA availability for the biosynthesis of the eugenin-precursor, 5,7-dihydroxy-2-methylchromone (Milke et al., 2019).

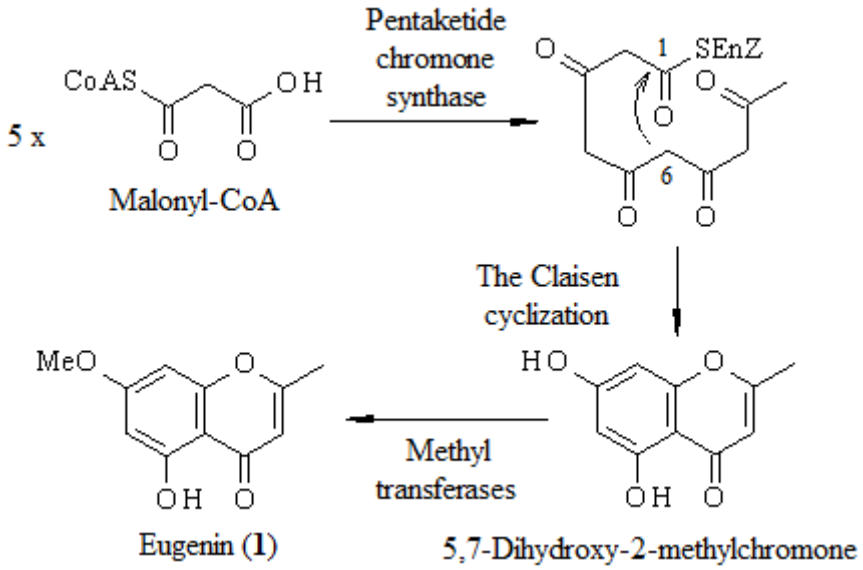

Fig. 2 Schematic diagram of the plausible biosynthesis of eugenin (**1**) in plants

Previously, Sarker and Phan (1975), using feeding of radioactive tracers, studied the biosynthesis of eugenin (**1**) in carrot root tissues induced by ethylene. ^{14}C-labelled acetate, malonate and acetoacetate were used as marking substrates, but acetate was found to be readily incorporated into eugenin (**1**) (**Fig. 3**). It was argued that if eugenin (**1**) was formed from acetate via polyketomethylene chain, the addition of the methyl functionality on C-1 could happen at the open polyketone chain stage or after cyclization; the latter would produce 5,7-dihydroxy-2-methylchromone, which is the biosynthetic precursor of eugenin (**1**). The results suggested that eugenin (**1**) biosynthesis could involve the acetate pathway with 5,7-dihydroxy-2-methylchromone as the precursor, in line with the previously described route to chromone nucleus formation (Egger, 1962; Chen et al., 1969). The effect of elicitation on the production of eugenin (**1**) in undifferentiated *Pimpinella anisum* L. cell cultures was studied, and it was observed that the solicitation with methyl jasmonates could enhance chromone accumulation in the medium (Soto-Argel et al., 2018). Similarly, the application of 2,6-dimethyl-β-cyclodextrins to the cell cultures could result in an increased (as much as 50-fold) accumulation of eugenin (**1**), which accumulated extracellularly after optimal elicitation conditions.

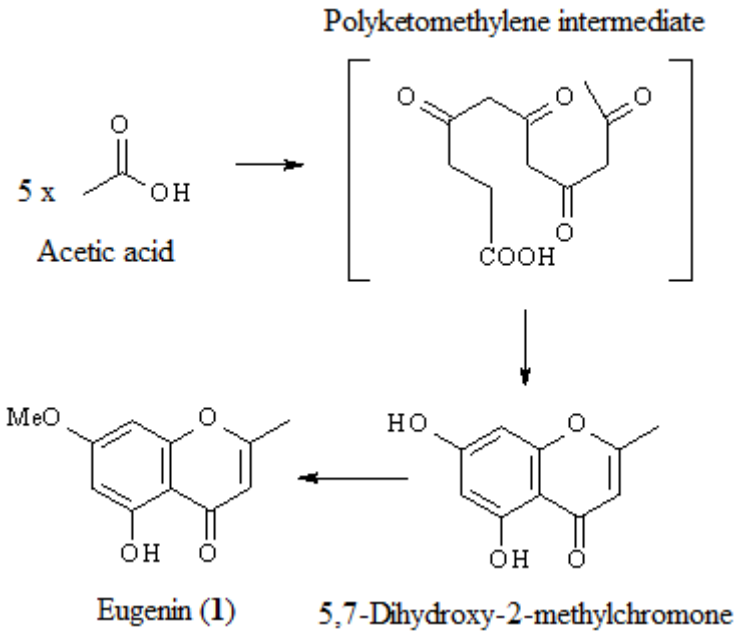

Fig. 3 Schematic diagram of the plausible biosynthesis of eugenin (**1**) in carrot root as demonstrated by Sarkar and Phan (1975)

4. Bioactivity

4.1 Antimalarial activity

There are two reported studies on the antimalarial activity of eugenin (**1**) as indicated by the anti-plasmodial activity (Tuntiwachuttikul et al., 2006; Sadorn et al., 2020). The *in vitro* anti-plasmodial activity assay (Trager and Jensen, 1976) was conducted with continuously cultured *Plasmodium falciparum* (K1, multidrug-resistant strain) and using the microculture radioisotope technique (Desjardins et al., 1979). However, both studies revealed no or a low level of activity against *P. falciparum* (EC_{50} = >20 μg/mL; IC_{50} = >48.5 μM). It can be mentioned that none of these studies was a focused and detailed antimalarial screening but was simply a part of preliminary bioactivity testing of certain plants/fungal extracts and their isolated compounds; eugenin (**1**) was just one of several isolated compounds. Nonetheless, even a low level of activity against the multidrug-resistant strain of *P. falciparum* could be significant, as it reveals the potential of eugenin (**1**) as a template to produce structural analogues to enhance the antimalarial potency for antimalarial drug development.

4.2 Antimicrobial activity

Tuntiwachuttikul et al. (2006) investigated the antibacterial potential of eugenin (**1**) against *Mycobacterium tuberculosis* H37Ra using the Microplate Alamar Blue Assay (MABA) (Collins and Franzblau, 1997), and the MIC (minimum inhibitory concentration) value was found to be 100 μg/mL. Later, a more detailed antimicrobial screening was performed with this chromone, isolated from the pathogenic fungal strain *Aschersonia confluens* BCC53152 (Sadorn et al., 2020). The antibacterial activity was assessed against *M. tuberculosis* H37Ra and other bacterial strains, i.e., *Acinetobacter baumannii*, *Bacillus ceresus, Enterococcus faecium, Escherichia coli, Klebsiella pneumoniae* and *Pseudomonas aeruginosa* and a fungal strain *Candida albicans.* A low level of bactericidal activity was observed against *M. tuberculosis* H37Ra (MIC = >50 μg/mL) and *Candida albicans* (MIC = >242.5 μM), whereas a low to moderate level (MIC = >25-50 μg/mL) of activity was found against both Gram-positive and Gram-negative microorganism including *A. baumannii*, *B. ceresus, E. faecium, E. coli, K. pneumoniae* and *P. aeruginosa.* In this study, while the green fluorescent protein microtitre assay (GFPMA) (Changsen et al., 2003) was utilized to assess the anti-*Mycobacterium* activity against *M. tuberculosis* H37Ra, the resazurin assay (Sarker et al., 2007) was applied for the determination of antimicrobial activity against the other microbial strains.

Table 4. Bioactivities of eugenin (**1**)

Type of bioactivity	Description	References
Antimalarial activity	Low level of inhibitory activity against *Plasmodium falciparum* (IC_{50} = >48.5 μM).	Sadorn et al., 2020
	No significant anti-plasmodial activity (EC_{50} = >20 μg/mL)	Tuntiwachuttikul et al., 2006
Antimicrobial activity	Low level of inhibitory activity against *Micrococcus tuberculosis* H37Ra (MIC = >50 μg/mL), and *Candida albicans* (MIC = >242.5 μM). Low to moderate levels (MIC = >25-50 μg/mL) of activity against other bacterial strains, e.g., *Acinetobacter baumannii*, *Bacillus ceresus, Enterococcus faecium, Escherichia coli, Klebsiella pneumoniae* and *Pseudomonas aeruginosa*	Sadorn et al., 2020
	Low level of inhibitory activity against *Mycobacterium tuberculosis* (MIC = 100 μg/mL)	Tuntiwachuttikul et al., 2006
Antioxidant	Eugenin (a phenolic antioxidant, **1**) content (TPC 13.51 mg GAE/g; TFC 223.20 mg RUE/g) was found to be highest at the full red stage of chili, which had the highest level of antioxidant activity as determined by the FRAP and radical scavenging activities, e.g., ABTS and DPPH	Yap et al., 2023
Antiplatelet aggregation activity	Strong antiplatelet aggregation activity *in vitro*. Platelet aggregation induced by thrombin, arachidonic acid, collagen, and platelet-activating factor was reduced to 76.4, 0, 18.2 and 65.4%, respectively.	Chen et al., 1996

Antiviral effect	*In silico* studies for potential anti-COVID-19 activity (against SARS-CoV-2 protease). Binding energy with COVID-19 target protein, obtained from docking study was -19.92 kcal/mol for eugenin (**1**).	Saraswat et al., 2021
Cytotoxic activity	Low level of cytotoxicity (IC_{50} = >242.5 μM) against the cell lines, MCF-7, KB, NCI-H187 and Vero.	Sadorn et al., 2020
	Significant activity against A-549, MCF-7 and HT-29 cell lines with GI_{50} values of 14, 10 and 25 μM, respectively.	Klausmeyer et al., 2009
Immunosuppressive/ immunomodulatory activity	Cytotoxicity against human peripheral blood T cells (68% survival at 25 μg/mL); Inhibition of IL-2 secretion (95% inhibition with 25 μg/mL).	Chang et al., 2003
	Pro-inflammatory cytokines TNF-alpha and IL-1 inhibitory activity. Therapeutic potential against rheumatoid arthritis as determined by *in vivo* and *in silico* studies. Weak inhibitory activity with 11.12% inhibition.	Xu et al., 2018
Osteogenesis-inducing effect	A low level of osteogenesis-inducing effect (*ca.* 50% compared to that of the positive control).	Lee et al., 2023
PEP-inhibitory activity	Weak activity (<10% inhibition).	Han and Paik, 2010
Blue-green algae growth inhibitory activity	Significant growth inhibitory activity against the blue-green algae *Microcystis aeruginosa* (IC_{50} = 1.6 μM) and *Anabaena floss-aquae* (IC_{50} = 2.8 μM).	Saito et al., 1989

A-549 = Lung cancer cell line; ABTS = 2,2'-Azino-bis(3-ethylbenzothiazoline-6-sulfonic acid); DPPH = 2,2-Diphenyl-1-picrylhydrazil; FRAP = Ferric reducing antioxidant power; EC = Effective concentration; GAE = Gallic acid equivalent; GI = Growth inhibition; HT-29 = Colon cancer cell line; IL = Interleukin; KB = Keratin forming tumour cell line; MCF-7 = Breast cancer cell line; NCI-H187 = Lung cancer cell line; PEP = Prolyl endopeptidase; RUE = Rutin equivalent; TFC = Total flavonoid content; TNF-alpha = Tumour necrosis factor alpha; TPC = Total phenolic content; Vero = Immortalized cell line established from kidney epithelial cells of the African green monkey

4.3 Antioxidant activity

Eugenin (**1**) is a phenolic compound, and like other phenols/polyphenols, this compound is expected to possess antioxidant property. In a recent study to determine the antioxidant property of chilies at different stages of development (green - red), it was observed that the chillies when they reach the red stage showed potent antioxidant activity as determined by the FRAP, ABTS and DPPH assays (Yap et al., 2023). The UPLC (ultra-performance liquid chromatography)-based chemical analysis revealed that the chilies when they are red had the highest level of eugenin (**1**), which could be linked to the antioxidant activity of the red chilies (Yap et al., 2023).

4.4 Antiplatelet aggregation activity

Among the bioactivities tested for eugenin (**1**), the antiplatelet aggregation activity of this compound is the most potent. A strong antiplatelet aggregation activity of eugenin (**1**) was observed *in vitro* (Chen et al., 1996). It was found that the platelet aggregation induced by thrombin, arachidonic acid, collagen, and platelet-activating factor was reduced to 76.4, 0, 18.2 and 65.4%, respectively, by this chromone. This finding could have some clinical implications as compounds that reduce platelet aggregation could be used to prevent or reverse platelet aggregation in arterial thrombosis, especially in myocardial infarction and ischaemic stroke (Born and Patrono, 2006). However, *in vivo* studies, including pre-clinical and clinical studies, are required before this chromone could be indicated as a therapeutically relevant antiplatelet aggregation agent.

4.5 Antiviral activity

Another important bioactivity of eugenin (**1**), as determined by the *in silico* work, is its activity against the SARS-CoV-2 virus and its therapeutic potential in the treatment of COVID-19 (Saraswat et al., 2021). The blind docking of various classes of compounds including control antiviral drugs, e.g., abacavir, acyclovir, quinoline and hydroxyquinoline), antimicrobial drugs e.g., levofloxacin, amoxicillin, cloxacin and ofloxacin, natural products e.g., amentoflavone, curcumin, eugenin (**1**), lycorine, myricetin, palmatine, saikosaponins and silymarin, was carried out. It was found that active compounds, including eugenin (**1**) (binding energy -19.93 kcal/mol), could successfully bind to the active site or near a crucial site of CoV-2 protease. Eugenin (**1**) was found to be one of the best five hits in terms of binding to the active site. Some physical parameters, e.g., molecular weight of 916.5, lipophilicity (logP) of 2.08, moderate water solubility, together with GI (gastro-intestinal) absorption and permeability could be

favourable for its potential as an anti-COVID-19 agent. The *in silico* ADMET study revealed low toxicity of eugenin (predicted LD_{50} = 1000 mg/kg). Taking all these into account, eugenin (**1**) seems to be an excellent candidate for anti-COVID-19 drug discovery and development. However, the results from this *in silico* predictive work must be substantiated with appropriate *in vitro* and *in vivo* studies, and eventually well-structured preclinical and clinical studies before eugenin (**1**) can be considered a true anti-COVID-19 agent.

4.6 Cytotoxicity

Cytotoxicity against cancer/tumour cell lines could be indicative, but not definitive, of the anticancer potential of any compound. Klausmeyer et al. (2009) reported a moderate level of cytotoxicity of eugenin (**1**) against three human cancer cell lines, i.e., A-549 (lung cancer), MCF-7 (breast cancer) and HT-29 (colon cancer), with the GI_{50} values of 14,10 and 25 μM, respectively, as determined by the MTT assay. Later, a low level (IC_{50} = >242.5 μM) of cytotoxicity of this chromone was described against MCF-7, KB (keratin forming tumour), NCI-H187 (lung cancer) and Vero (noncancerous immortalized cell line established from kidney epithelial cells of the African green monkey) cell lines (Sadorn et al, 2020). While the cytotoxic activity of eugenin (**1**) against a few human cancer cell lines was not strong and may not have any clinical relevance concerning cancer, this compound could be used as a template to generate various structural analogues by simple functional group modification and/or addition of new pharmacophores in the core skeleton to enhance its cytotoxicity.

4.7 Immunosuppressive/immunomodulatory activity

Immunosuppressive activity can be defined by the ability of any compound or drug (e.g., corticosteroids) to inhibit or prevent the activity of the immune system. Immunosuppression induced by a drug is desired especially in the preparation of bone marrow or other organ transplantation to prevent rejection of the donor tissue (Wiseman, 2016). Immunosuppressive agents are also commonly used in the treatment of autoimmune and immune-mediated diseases. The immunosuppressive activity of eugenin (**1**) was reported by Chang et al. (2003). It was observed that this compound could significantly inhibit IL-2 (interleukin-2) secretion (95% inhibition with a dose of 25 μg/mL) and potently inhibit CD28-costimulated activation of human peripheral blood T cells without any significant cytotoxicity towards the human peripheral blood T cells (68% survival at 25 μg/mL) as determined by the MTT assay. A 50% inhibition of IL-2 secretion was achieved by only 5 μg/mL of eugenin (**1**). It can be noted that IL-2 is an immunostimulatory factor that supports the expansion of

activated effector T cells (Pol et al., 2020). The immunosuppressive activity of eugenin (**1**) has therapeutic potential against autoimmune disease, albeit further *in vivo* studies including preclinical and clinical trials are necessary to firmly establish this potential.

Earlier, Xu et al. (2018) reported the TNF-alpha (tumour necrosis factor alpha) and IL-1 (interleukin-1) inhibitory activity of eugenin (**1**), and evaluated its therapeutic potential against rheumatoid arthritis, which is an autoimmune and inflammatory disease, by *in vivo* and *in silico* studies. A weak inhibitory activity with 11.12% inhibition was observed.

4.8 Osteogenesis-inducing activity

Eugenin (**1**), isolated from *P. multiflorus* var. *albus* fruits, has recently been evaluated for its regulatory effects on the differentiation between osteogenesis and adipogenesis of mesenchymal stem cells. In this study, a low level of osteogenesis-inducing activity (*ca.* 50% compared to that of the positive control) has been reported for eugenin (**1**) (Lee et al., 2023). However, the level of activity was too low to be considered for any therapeutic applications.

4.9 PEP-inhibitory activity

Eugenin (**1**) was found to display weak prolyl endopeptidase (PEP)-inhibitory activity (<10% inhibition), which was assessed using benzyloxy-carbonyl-glycyl-L-propyl-*p*-nitroanilide as a substrate and by determining the amount of released *p*-nitroaniline at 380 nm (Han and Paik, 2010). It can be noted that the PEP-inhibitory activity of any compound can highlight its potential use against memory impairment and cognitive decline.

4.10 Blue-green algae growth inhibitory activity

Significant growth inhibitory activity against the blue-green algae *Microcystis aeruginosa* (IC_{50} = 1.6 μM) and *Anabaena floss-aquae* (IC_{50} = 2.8 μM) (Saito et al., 1989). Although this bioactivity might not have any therapeutic relevance, it has some ecological significance. This study indicated that eugenin (**1**) could potentially be used for the improvement of water quality. It can be noted that the blue-green algae breed in eutrophicated water and often constitute water bloom, which affects the water quality, and some species of these algae contain cyclopeptides which are toxic to fish and mammals (Botes et al., 1984; Botes et al., 1985; Watanabe et al., 1986).

5. Conclusion

The distribution of eugenin (**1**) is rather limited to a few plant families and only a couple of fungal species. Based on the reported bioactivities, it could be concluded that this chromone may have some potential as a template for new drug development, particularly, for the treatment of COVID-19, and as an antiplatelet aggregation and immunosuppressive/immunomodulatory agent.

Acknowledgement

Lutfun Nahar gratefully acknowledges the financial support of the European Regional Development Fund - Project ENOCH (No. CZ.02.1.01/0.0/0.0/16_019/0000868) and the Czech Agency Grant - Project 23-05474S.

References

Aeri, V., Narayana, D. B. A., Singh, D., 2020. *Syzygium cumini*, in "Powdered Crude Drug Microscopy of Leaves and Barks", Elsevier, pp. 119-122.

Ajiboye, T. O., Mohammed, A. O., Bello, S. A., Yusuf, I. I., Ibitoye, O. B., Muritala, H. F., Onajobi, I. B., 2016. Antibacterial activity of *Syzygium aromaticum* seed: Studies on oxidative stress biomarkers and membrane permeability. Microb. Pathogenesis 95, 208-215.

Al-Douri, N. A., Dewick, P. M., 1988. Biosynthesis of the 3-ethylchromone phytoalexin lathodoratin in *Lathyrus odoratus*. Phytochemistry 22, 775-783.

Ali, A., Makboul, M., Attia, A., Ali, D. Chromones and flavans from *Pancratium maritimum*. Phytochemistry 29, 625–627.

Anh, D. T. P., Duong, T. B., Hoang, V. D., 2014. A new chromone from *Hymenocallis littoralis* Salisb. (Amaryllidaceae). Nat. Prod. Res. 28, 1869-1872.

Arafa, A. M., Abdel-Ghani, A. E., El-Dahmy, S. I., Abdelaziz, S., 2020. Micropropagation, myristicin production enhancement, and comparative GC-MS analysis of the n-hexane extracts of different organs of *Daucus pumilus* (Gouan) family Apiaceae. J Pharm Bioallied Scs, 12, 324-334.

Born, G., Patrono, V., 2006. Antiplatelet drugs. Br. J. Pharmacol. 147, S241-S251.

Botes, D. P., Tuinman, A. A, Wessels, H., Viljoen, C. C., Kruger, H., Williams, D. H., Santikarn, S., Smith, R. J., Hammond, S. J., 1984. The structure of cyanoginosin-LA, a

cyclic heptapeptide toxin from the cyanobacterium *Microcystis aeruginosa*. J. Chem. Soc., Perkin Trans. 1, 2311-2318.

Botes, D. P., Wessels, H., Kruger, H., Runneger, M. T. C., Santikarn, S., Smith, R. J., Barna, J. C. J., Williams, D. H., 1985. Structural studies on cyanoginosins-LR, -YR, -YA, and YM, peptide toxins from *Microcystis aeruginosa*. J. Chem. Soc., Perkin Trans. 1, 2747-2748.

Chang, W. L., Chiu, L. W., Lai, J. H., Lin, H. C., 2003. Immuno suppressive flavones and lignans from *Bupleurum scorzonerifolium.* Phytochemistry 64, 1375-1379.

Changsen, C., Franzblau, S. G., Palittapongarnpim, P., 2003. Improved green fluorescent protein reporter gene-based microplate screening for antituberculosis compounds by utilizing an acetamidase promoter. Antimicrob. Agents Chemother. 47, 3682-3687.

ChEBI, 2023. Chemical Entities of Biological Interest, a freely available dictionary of molecular entities focused on 'small' chemical compounds. Available online at: https://www.ebi.ac.uk/chebi/chebiOntology.do?chebiId=CHEBI:67374, accessed on 22 July 2023.

Chen, M., Stohs, S. J., Staba, E. J., 1969. The biosynthesis of visnagin from 2-^{14}C-acetate by *Ammi visnaga* suspension cultures and the metabolism of ^{14}C-vistiagin and ^{14}C-khellin by *A. visnaga* and *A. majus*. Lloydia 32, 339-346.

Chen, I. S., Chang, C. T., Sheen, W. S., Teng, C. M., Tsai, I. L., Duh, C. Y., Ko, F. N., 1996. Coumarins and antiplatelet aggregation constituents from Formosan *Peucedanum japonicum*. Phytochemistry 41, 525-530.

Collins, L., Franzblau, S. G., 1997. Microplate alamar blue assay versus BACTEC 460 system for high-throughput screening of compounds against *Mycobacterium tuberculosis* and *Mycobacterium avium*. Antimicrob. Agents Chemother., 41, 1004-1009.

Coxon, D. T., Curtis, R. F., Price, K. R., Levett, G., 1973. Abnormal metabolites produced by Daucus carota roots stored under conditions of stress. Phytochemistry 12, 1881-1885.

Czepa, A., Hofmann, T., 2003. Structural and sensory characterization of compounds contributing to the bitter off-taste of carrots (*Daucus carota* L.) and carrot puree. J. Agric. Food Chem. 51, 3865-3873.

Desjardins, R. E., Canfield, C. J., Haynes, J. D., Chulay, J. D., 1979. Quantitative assessment of antimalarial activity in vitro by a semiautomated microdilution technique. Antimicrob. Agents Chemother. 16, 710-718.

Egger, K., 1962. Zur Biogenese von Khellol in *Eranthis hiemalis* L. Planta 58, 326-332.

Fujita, R., Fujita, T., Suzuki, T., 1967. On the constituents of *Nauclea orientalis* L. I. Noreugenin and naucleoside, a new glycoside (terpenoids V). Chem. Pharm. Bull. 15, 1682-1686.

Han, A. R., Paik, Y. S., 2010. Acetophenone glucosides from the clove buds (*Syzygium aromaticum*). J. Korean. Soc. Applied Biol. Chem. 53, 847-851.

Hauser, D., Zardin, T., 1972. Isolation of 6-hydroxymethyl-eugenin from *Chetomium minutum.* Experientia 28, 1114-1115.

Kayed, A. M., Genady, E. A. M., Kadry, H. A., Elghaly, E. M., 2021. New phytoconstituents, antimicrobial and cytotoxic activities of *Acacia etbaica* Schweinf. Nat. Prod. Res. 35, 5571-5580.

Klausmeyer, P., Scudiero, D. A., Uranchimeg, B., Melillo, G., Cardellina, J. H., Shoemaker, R. H., Chang, C. J., McCloud, T. G., 2009. Cytotoxic and HIF-1 alpha inhibitory compounds from *Crossosoma bigelovii.* J. Nat. Prod. 72, 805-812.

Lee, Y. H., Hong, J. H., Patk, K. H., Kim, S. H., Kim, J. C., Kim, D., Park, Y. H., Lee, K. W., Kim, J. K., Kim, K. H., 2023. Phytochemical investigation of bioactive compounds from white kidney beans (fruits of *Phaseolus multiflorus* var. *albus*): Identification of denatonium with osteogenesis-inducing effect. Plants 10, article number: 2205.

Meijer, T. M., Schmid, H., 1948. On the constitution of eugenin. Helv. Chim. Acta 31, 1603-1607.

Milke, L., Kallscheuer, N., Kappelmann, J., Marienhagen, J., 2019. Tailoring *Corynebacterium glutamicum* towards increased malonyl-CoA availability for efficient synthesis of the plant pentaketide noreugenin. Microbial Cell Factories 18, article number: 71.

Morita, H., Abe, I., Noguchi, H., 2010. Plant type III PKS. In Comprehensive Natural Products II - Chemistry and Biology, Volume 1, Elsevier, pp, 171-225.

Najmuldeen, I. A., Ketuly, K. A., Hadi, A. H. A., 2013. Phenolic compound, triterpene and steroids from the leaves and bark of *Dysoxylum macrocarpum.* Journal of University of Zakho 1, 227-245.

Pol, J. G., Caudana, P., Paillet, J., Piaggio, E., Kroemer, G., 2020. Effects of interleukin-2 in immunostimulation and immunosuppression. J. Exp. Med., article number: e20191247.

PubChem, 2023. National Library of Medicine, National Center for Biotechnology Information. Available online at: https://pubchem.ncbi.nlm.nih.gov/compound/Eugenin

Rao, G-X., Wang, Y-H., Cai, F., Lin, Z-W., Sun, H-D., 1991. Chemical constituents from *Ligusticum pteridophyllum.* Acta Bot. Yunnanica 13, 233-236.

Sadorn, K., Saepua, S., Punyain, W., Saortep, W., Choowong, W., Rachtawee, P., Pittayakhajonwut, P., 2020. Chromanones and aryl glucoside analogs from the entomopathogenic fungus *Aschersonia confluens* BCC53152. Fitoterapia 144, article number: 104606.

Saito, K., Matsumoto, M., Sekine, T., Murakoshi, I., Morisaki, N., Iwasaki, S., 1989. Inhibitory substances from *Myriophyllum brasiliense* on growth of blue-green-algae. J. Nat. Prod. 52, 1221-1226.

Saraswat, J., Singh, P., Patel, R., 2021. A computational approach for the screening of potential antiviral compounds against SARS-CoV-2 protease: Ionic liquid vs herbal and natural compounds. J. Mol. Liq. 326, article number: 115298.

Sarkar, S. K., Phan, C. T., 1975. The biosynthesis of 8-hydroxy-6-methoxy-3-methyl-3,4-dihydroisocoumarin and 5-hydroxy-7-methoxy-2-methylchromone in carrot root tissues treated with ethylene. Physiol. Plant 33, 108-112.

Sarkar, S. K., Phan, C. T., 1975. Naturally occurring and ethylene-induced phenolic compounds in the carrot root. J. Food Protection 42, 526-534.

Sarker, S. D., Nahar, L., Kumarasamy, Y., 2007. Microtitre plate-based antibacterial assay incorporating resazurin as an indicator of cell growth, and its application in the *in vitro* antibacterial screening of phytochemicals. Methods 42, 321-324.

Schlittler, E., Spitaler, U., 1978. Contents of *Schumanniphyton problematicum.* Tet. Lett. 32, 2911-2914.

Soto-Argel, C., Hidalgo, D., Palazon, J., Corchete, P., 2018. Extracellular chromone derivatives in cell cultures of *Pimpnella anisum.* Influence of elicitation with methyl jasmonates and 2β-methyl cyclodextrins. Biotechnol Lett 40, 413-418.

Stoessl, A., Stothers, J. B., 1978. post-infectional inhibitors from plants.32. C-13 biosynthetic study of stress metabolites from carrot roots: Eugenin and 6-methoxymellein. Can. J. Bot. 56, 2589-2593.

Trager, W., Jensen, J. B., 1976. Human malaria parasites in continuous culture. Science 193, 673-675.

Tsui, W-Y., Brown, G. D., 1996. Chromones and chromanones from *Baeckea frutescens.* Phytochemistry 43, 871-876.

Tuntiwachuttikul, P., Phansa, P., Pootaeng-On, Y., Taylor, W. C., 2006. Chromones from the branches of *Harrisonda perforata*. Chem. Pharm. Bull. 54, 44-47.

Vickery, M. L., Vickery, B., 1981. The Acetate-Malonate Pathway. In: Secondary Plant Metabolism. Palgrave, London.

Wang, D. Y., Ye, Q., Li, B. G., Zhang, G. L., 2003. A new anthraquinone from *Gladiolus gandavensis.* Nat. Prod. Res. 17, 365-368.

Watanabe, Y., Watanabe, M. F., Watanabe, M., 1986. The distribution and relative abundance of bloom forming *Microcystis* species in several eutrophic waters. Jpn. J. Limnol. 47, 87-93.

Wiseman, A. C., 2016. Immunosuppressive medications. Clin. J. Am. Soc. Nephrol. 11, 332-343.

Xu, S. K., Peng, H., Wang, N., Zhao, M., 2018. Inhibition of TNF-alpha and IL-1 by compounds from selected plants for rheumatoid arthritis therapy: *In vivo* and *in silico* studies. Trop. J. Pharm. Res. 17, 277-285.

Yap, E. S. P., Uthairatanakiji, A., Lohakunjit, N., Jitareerat, P., Maier, C. S., 2023. Targeted and untargeted metabolites and antioxidant properties of chilli pepper at different maturity stages. Crop Sci. published online ahead of print, DOI: 10.1002/csc2.20967

Zhou, Q., 2000. Bioactive components from *Crossosoma bigelovii* and studies on novel selenophene-containing heteroarene compounds as anticancer agents. PhD thesis, Purdue University, USA.